Journal of Marine Research, 54, 521–540, 1996

The eastern boundary of the Gulf Stream recirculation

by Paul J. Marchese[1] and Arnold L. Gordon[1]

ABSTRACT

A meridionally aligned thermocline front near 60W in the subtropical North Atlantic is revealed by the 1992 Trident data set. The front separates saltier thermocline water to the east from less salty water to the west. The eastern water is subjected to excess evaporation of the subtropics, while the western water is fed by lower salinity Gulf Stream water, which derives water from the wet tropical Atlantic. It is suggested that the front marks the eastern edge of the Gulf Stream recirculation cell, hence refer to it as the recirculation front. The surface layer displays a fan-like T/S scatter above the 18°C Subtropical Mode Water, with the fresher surface water located west of the recirculation front, and a subsurface salinity maximum to the east. In the lower thermocline (8 to 12°C) there is a step-like salinity increase of about 0.04 toward the east as measured along isotherms, producing two modes in the T/S scatter. At the intermediate water level (approximately in the 4 to 8°C range) the extent of the low salinity Antarctic Intermediate Water and salty Mediterranean outflow water are also reflected in the position of the recirculation front. That the front marks the easternmost extent of the Gulf Stream recirculation is supported by the potential vorticity, which reveals a region of high homogeneous values within the recirculation cell. East of the front, the potential vorticity field is sloped along isopycnals indicating the meridional flow of the Sverdrup interior. Mapping of the recirculation front using archived data reveals that it extends deep into the subtropical convergence zone (STCZ), a region whose fronts have all been previously attributed to Ekman convergence.

1. Introduction

The concept of an anticyclonic Gulf Stream recirculation cell was first invoked by Worthington (1976) to explain the Gulf Stream transport which increased from 30 Sv (Sv = 1×10^6 m^3/s) through the Florida Straits to 150 Sv near Nova Scotia, followed by a decrease to 37 Sv before continuing east as the North Atlantic Drift. To maintain continuity Worthington proposed that some of the water that flows past Cape Hatteras turn south in an anticyclonic manner to add to the flow north of the Straits of Florida. The velocities within the recirculation gyre also have to be large to produce the transports observed.

The Gulf Stream recirculation cell concept increased the complexity of subtropical circulation patterns, which previously consisted of a single anticyclonic gyre com-

1. Lamont Doherty Earth Observatory, Palisades, New York, 10964, U.S.A.

posed of a sluggish southward flow in the interior, driven by wind stress curl as described by the Sverdrup relation, with a strong northward-flowing narrow western boundary current. The recirculation requires the inclusion of higher order dynamics to account for the small, energetic gyre in the western third of the subtropical regime. A cyclonic recirculation gyre located between the Grand Banks and the Gulf Stream has also been identified (Hogg *et al.,* 1986). Both recirculation cells have been observed using direct current measurements (Schmitz, 1980; Owens *et al.,* 1982; Owens, 1984, 1991; Richardson, 1985; and can be distinguished in maps of dynamic topography (Stommel *et al.,* 1978; Reid, 1994) although geostrophic calculations without explicit reference level information could be misleading because of a significant barotropic component in the recirculation cell (Stommel *et al.,* 1978).

Models suggest that the Gulf Stream recirculation cell is needed to balance negative vorticity that is either advected north by the western boundary current (Cessi *et al.,* 1987), or created by the vortex tube stretching which is associated with the formation of the Subtropical Mode Water (STMW; Huang, 1990; Spall, 1992). In both cases the dissipation of negative vorticity at the western boundary is insufficient and the recirculation provides a mechanism through which the excess vorticity can be removed. The recirculation increases the Gulf Stream transport without increasing the throughflow, which cannot exceed the combined Sverdrup and thermohaline transports. The increased flow, through its interaction with the topography (Csanady and Pelegri, 1995), provides the extra dissipation of negative vorticity.

The recirculation cell may have some impact on the thermohaline flow by altering the salinity of the thermocline waters that eventually feed North Atlantic Deep Water (NADW) production. The thermohaline component of the Gulf Stream throughflow does not have a direct route through the subtropical gyre as observed from the SOFAR float trajectories (Owens, 1984). Instead, the water is circulated several times within the recirculation gyre before continuing north. While in the recirculation, the water is subjected to mixing and high evaporation (Schmitt *et al.,* 1989). As a result, the water that eventually escapes the gyre is saltier than that which enters the Straits of Florida, facilitating the production of NADW.

The focus of recirculation cell studies has been associated with the transport in the western boundary; not as much attention has been given to defining the eastern extent of the gyre. In this paper we use water mass indicators to identify a front marking the eastern, seaward edge of the Gulf Stream anticyclonic recirculation cell.

2. Trident data

a. Data array. The Trident cruise of August 1992 aboard the NOAA research vessel *Malcolm Baldrige* carried out an oceanographic survey of the western trough of the subtropical North Atlantic. The data consisted of continuous vertical conductivity and temperature profiles using a Neil Brown Mark III CTD (conductivity, temperature and depth) profiler, and up to 24 ten liter Niskin bottles that were sampled for

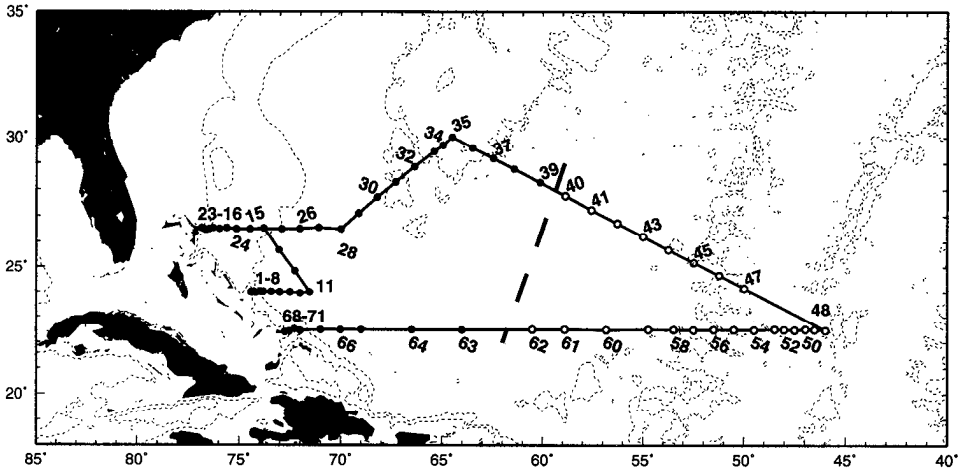

Figure 1. Trident 1992 cruise station map with 1000 and 3000 m isobaths. Stations east of the thermocline front are shown as open circles, those west as solid circles. The position of the front is shown as a dashed line.

salinity, oxygen, nutrients (silicate, phosphate, nitrate, nitrite), chloroflourocarbons (CFC's), and tritium/helium[3]. The CTD temperature and pressure sensors were calibrated under laboratory conditions before and after the cruise. The CTD-calculated salinity was calibrated against the bottle values. The hydrographic data have an accuracy of ±0.005°C for the temperature and ±.002 for the salinity. The cruise contains 71 stations (Fig. 1) which extend to the bottom. The stations along 22.5N, stations 48 through 71, are referred to as the southern section. Stations 14 through 48 define the northern section.

b. Northern section. The temperature and salinity data for the Trident sections were contoured and plotted (Figs. 2 and 3). For convenience the water above the 18°C isotherm is referred to as the upper thermocline, between 12 and 18°C is the main thermocline, and between 8 and 12°C is the lower thermocline. The intermediate water is found below the 8°C isotherm.

In the northern section, the STMW (18°C water) of the North Atlantic appears as a thermostad between the 18 and 19°C isotherms (Figs. 2a). This is slightly warmer than 17.9 ± 0.3°C, which is the characteristic temperature for this mode water (Worthington, 1959). The warming is not unexpected since the temperature of the STMW varies considerably with time as evidenced by the time series at the Panulirus station near Bermuda (Talley and Raymer, 1982). The STMW is most prominent between stations 32 and 39. This increase in thickness is the result of the more northern position of these stations and their proximity to the area of STMW formation (Worthington, 1972; McCartney, 1982). East of station 39, the mode water diminishes rapidly, though a weak thermostad extends to station 44.

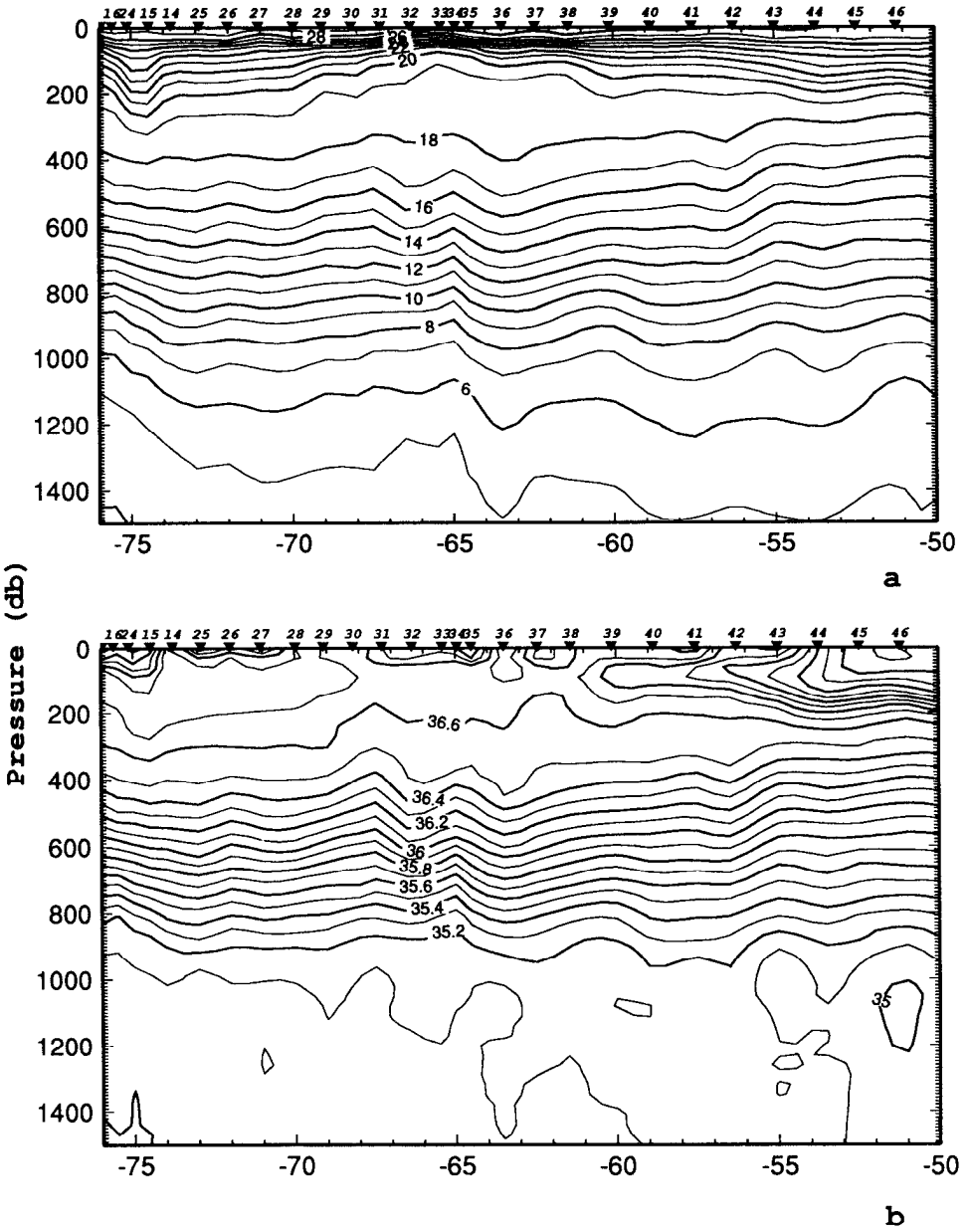

Figure 2. Potential temperature (a) and salinity (b) for the upper 1500 db of the northern section (stations 14 to 47).

Above the STMW the isotherms are compressed between stations 30 and 39 where the STMW is most conspicuous. Below the 18°C water and east of 73W, the isotherms generally shallow toward the east, except for the irregularities near 58 and 63W. West of 73W, the isotherms in the main and lower thermocline deepen to the east.

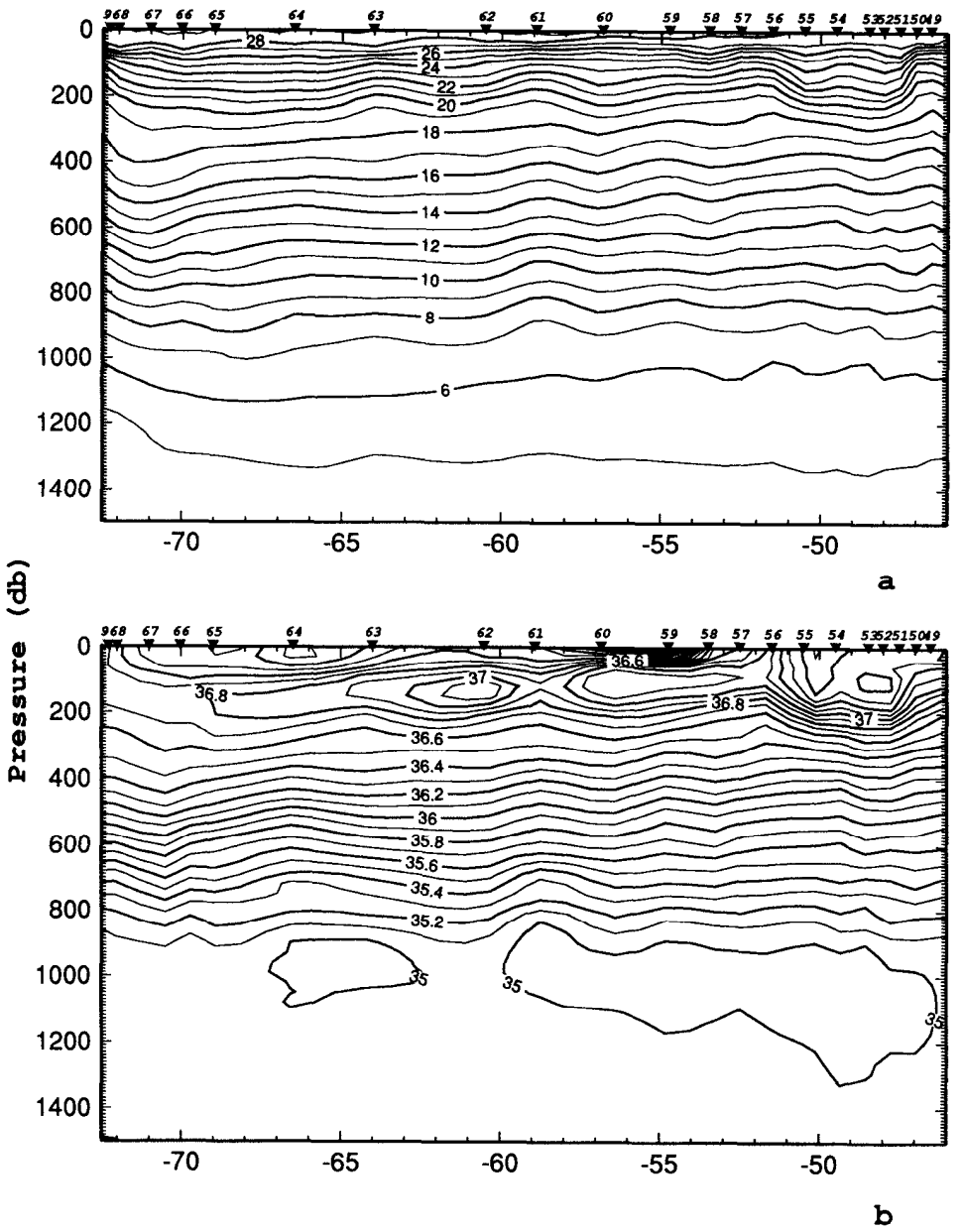

Figure 3. Potential temperature (a) and salinity (b) for the upper 1500 db of the southern section (stations 48 to 71).

A sense of the baroclinic shear can be derived by the inspection of the temperature since, to a large extent, the temperature field gives a good approximation of the isopycnal field. In the upper and main thermocline the baroclinic shear have opposite signs across most of the section except for the westernmost stations where the isotherms slope down toward the east throughout the thermocline. This implies a general northward geostrophic transport in the western edge of the section relative to a deep reference layer. The northward flow east of the Bahamas is what traditionally has been referred to as the Antilles Current (Sverdrup *et al.,* 1942; Gunn and Watts, 1982; Lee *et al.,* 1990).

The STMW can be distinguished in the salinity field (Fig. 2b) by a reduced vertical gradient between 200 and 400 decibars. A surface high salinity region is observed, east of station 44. The high surface salinity water (Worthington, 1976) results from the high evaporation and low precipitation in this area of the North Atlantic (Schmitt *et al.,* 1989). Protruding west from the high salinity water is a subsurface salinity maximum, *s*-max, which is referred to as subtropical underwater (STUW; Wüst, 1963; Gunn and Watts, 1982). The thicker stratum of STMW west of station 38 seems to block the westward intrusion of the saltier STUW, as the compression of the isopycnals above the STMW creates a density gradient and geostrophic shear that deflects the STUW into a more meridional bearing. At the surface salinity maximum water boundary, the roles are reversed so that the higher salinity water stops the eastward penetration of the STMW.

Below the STMW, the salinity has the same general shape seen in the isotherms. Below the thermocline (below roughly 900 db) the salinity for the most part falls between 35.0 and 35.1 marking the salinity minimum of the Antarctic Intermediate Water (AAIW). The saltier, warmer values in the intermediate layer indicate saline Mediterranean outflow water (Tsuchiya, 1989) which penetrates this section between 52 and 65W.

c. Southern section. In the southern section (Fig. 3) the STMW is barely evident. As a result the STUW intrudes farther west than in the northern section. The salinity maximum water is deeper in this section and is observed in the temperature field where a deepening of isotherms occurs between stations 50 and 56. As in the northern section, the temperature gradient at the western edge indicates a baroclinic shear with northward transport. In the main thermocline there is a gradual shallowing to the east of the isotherms and isohalines except for a step-like jump at station 61. At the intermediate water level the salinity does not exceed 35.1. Mediterranean water is not observed in this section.

d. Potential temperature-salinity (T/S) relationship. The *T/S* relationship reveals the various water masses dominating the western subtropical North Atlantic. A relatively abrupt transition in *T/S* characteristics between stations 39 and 40 and between 62

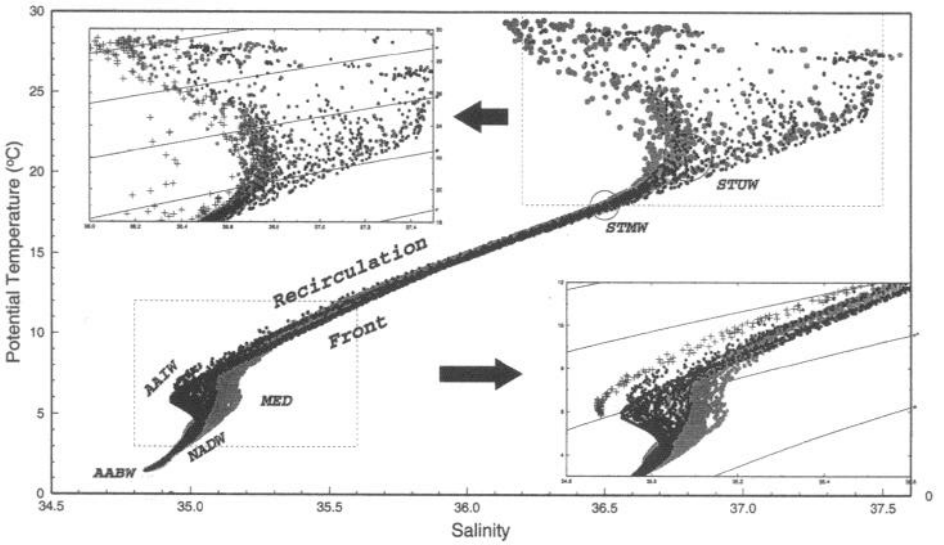

Figure 4. Potential temperature vs. salinity plot for the northern (gray) and southern (black) sections. The boxed inserts focus on the upper and lower thermocline water and include the Straits of Florida data (crosses) for the Atlantis II, 1981 cruise (Roemmich and Wunsch, 1985).

and 63, near 60W suggests the presence of a front within the thermocline to intermediate water. From the 18°C STMW thermostad to approximately 15°C the T/S characteristic for both sections (Figs. 4, 5, 6) is remarkably uniform. The water layers both shallower and deeper than the 15° to 18°C stratum display a wider range of T/S characteristics, suggesting a more complex intermingling of water masses for the near surface layer and lower thermocline.

In the western edge of both sections the surface water is relatively less saline (Figs. 5a, 6a). This is particularly evident in the northern section which has a fresher component not observed in the south. This westernmost water of the northern section has properties similar to Florida Straits throughflow (Fig. 4) which is drawn from the high precipitation regions of the tropics (Schmitz and Richardson, 1991). This implies that the Antilles Current freshens as it mixes with the Florida Straits water north of the Bahamas to eventually form the Gulf Stream. Toward the east, the surface salinity increases rather abruptly at the front near 60W. Both sections reveal two families of curves in T/S space for the lower thermocline (Figs. 5b, 6b). The saltier lower thermocline water falls east of the 60W front. The fresher lower thermocline water is to the west.

Below the 8°C isotherm, the intensity of the AAIW s-min is modified by more saline water derived from the Mediterranean Sea outflow (Kawase and Sarmiento, 1986). In the northern section the s-min near 6°C occurs in the southernmost stations (45 through 48) which are south of the high salinity Mediterranean water tongue

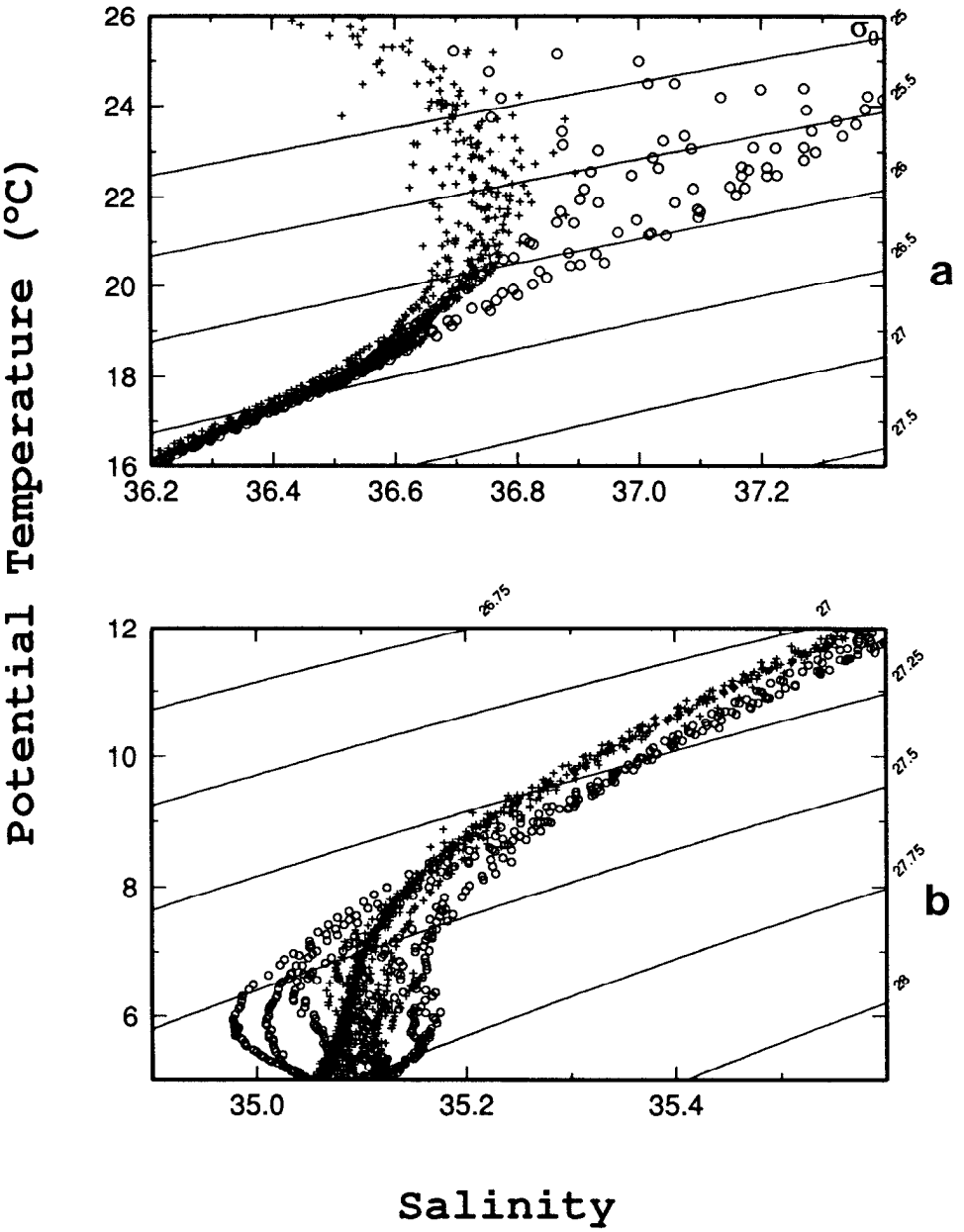

Figure 5. Potential temperature vs. salinity for the northern section. Focuses on the upper (a) and lower (b) thermocline. The stations east of the recirculation front are marked with open circles. Those stations west of the front are marked by crosses. The front as observed from the gap in the scatter occurs between station 39 and 40.

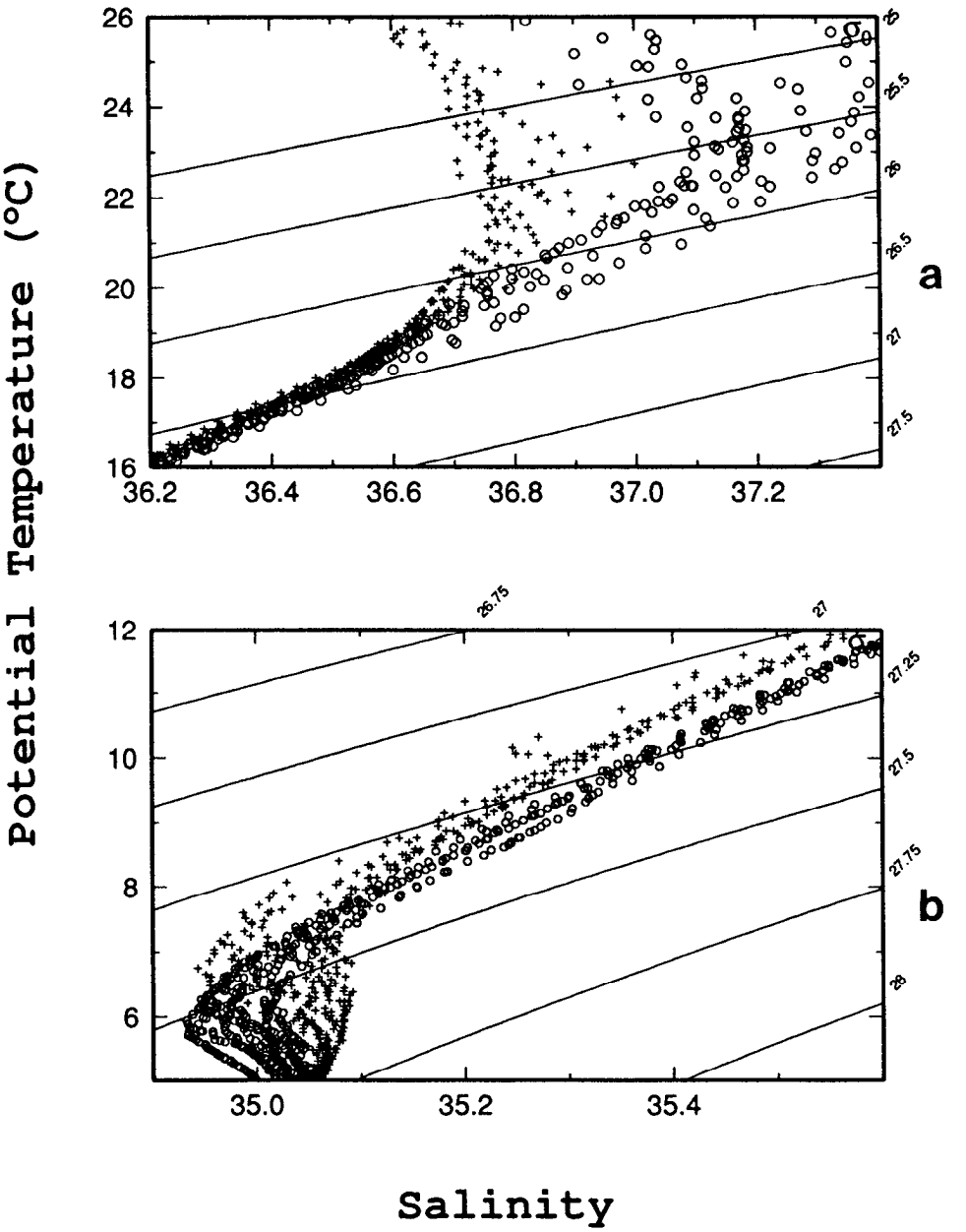

Figure 6. Potential temperature vs. salinity for the southern section. Focuses on the upper (a) and lower (b) thermocline. The stations east of the recirculation front are marked with open circles. Those stations west of the front are marked by crosses. The front occurs between station 62 and 63.

(Worthington, 1976) contained in stations 35 through 44. In the southern section (Fig. 6b) the AAIW *s*-min is fresher than in the north because of the reduced influence of the Mediterranean water outflow. As in the thermocline, an abrupt change in T/S properties is observed near 60W. The stations west of the front contain a *s*-min at temperatures close to 7°C, whereas east of the front the main *s*-min of the AAIW core is closer to 6°C.

Below the intermediate waters are the NADW and Antarctic Bottom Waters (AABW). The change near 2°C in the T/S slope marks the transition between these two deep water masses (Wright, 1970; Broecker *et al.,* 1976). No trace of a front is observed in the deep and bottom water masses.

3. The recirculation front

a. Identification. To briefly summarize the above: the Trident data reveal the existence of a meridionally aligned thermocline front near 60W. The front is particularly prominent in the upper and lower thermocline where a bimodal distribution in the water properties is seen in T/S coordinates. Above the Subtropical Mode Water, the T/S scatter has a fan-like shape with the saltier waters located to the east of 60W. In the lower thermocline (8 to 12°C) the T/S scatter is bimodal, with saltier water also to the east. We believe that the thermocline front marks the eastern edge of the Gulf Stream recirculation cell.

The salinity distributions on isopycnal surfaces shallower than the STMW reveal a high salinity region centered at 40W, 20N (Fig. 7a), the source of the surface salinity maximum and STUW *s*-max. High salinity in this region is induced by the excess evaporation (Schmitt *et al.,* 1989) compounded by the long residence time of the sluggish interior circulation. Two prongs of salty upper thermocline water extend westward at 19N and 27N. The defining feature may be the lower salinity west of 60W in the 20 to 27S band, which we suggest is a product of the lower salinity Gulf Stream recirculation cell water.

In the lower thermocline (Fig. 7c) the highest salinity is found in the eastern subtropical North Atlantic. This pattern reflects the circulation expected within the ventilated thermocline (Luyten *et al.,* 1983), with southward advection from Ekman induced subduction in the northern region of the subtropical gyre. The surface salinity at 50N, where the 27.2 density layer outcrops, is comparable to the values observed at depth. Some salinity enhancement may be forced by vertical mixing with the saltier, deeper Mediterranean water. The high salinity intrudes farther west near 27N, just as in the upper thermocline (Fig. 7a).

The property maps explain many of the features observed in the T/S plots. In the upper and lower thermocline the variation in the salinity results because of the high salinity intrusion in the east. In the main thermocline there is no high salinity signal in the east (Fig. 7b) explaining the tightening of the T/S properties between 15 and 18°C.

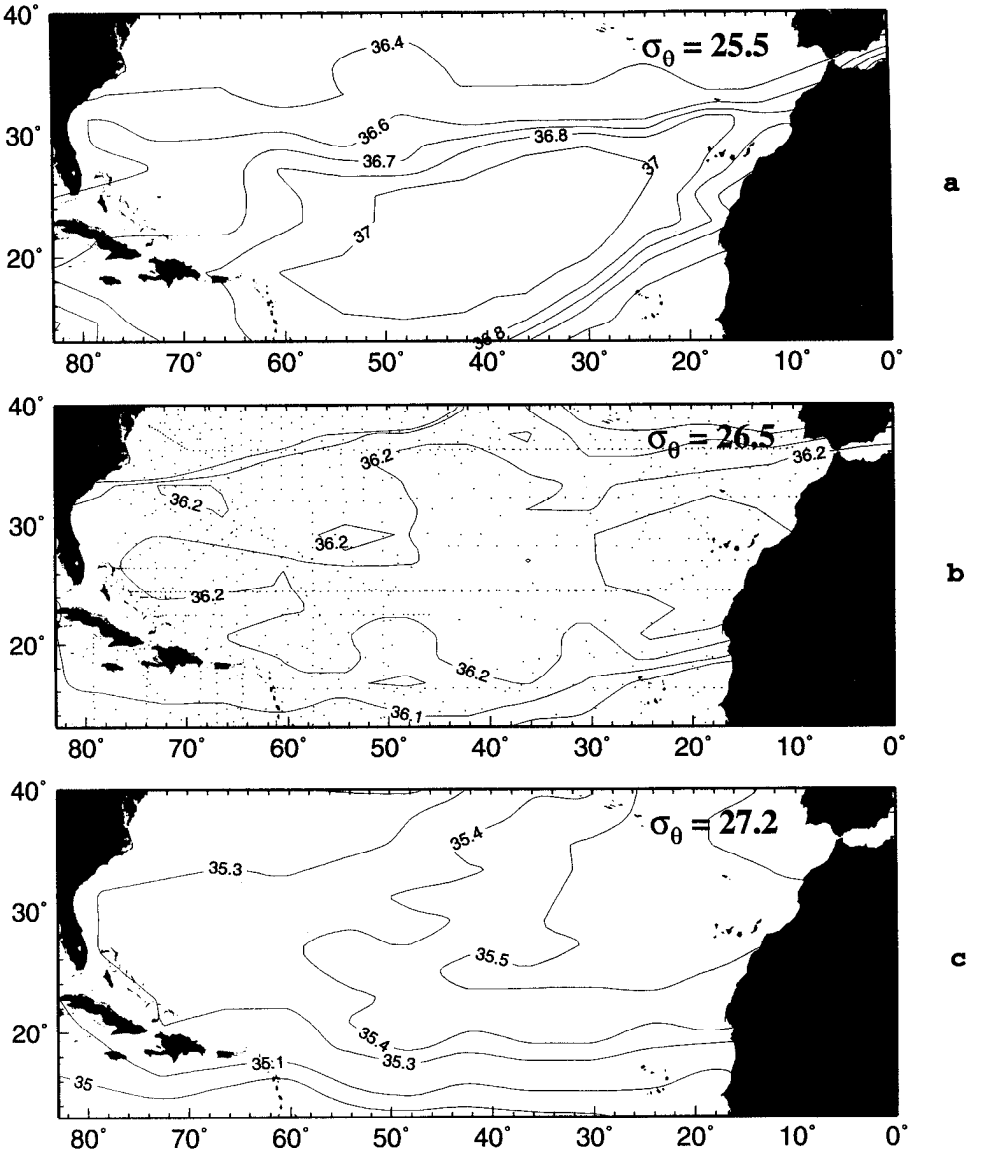

Figure 7. Salinity distribution of the subtropical North Atlantic on isopycnal surfaces: σ_θ = 25.5 (a), σ_θ = 26.5 (b), σ_θ = 27.2 (c). Constructed from the "Reid data set" (Reid, 1994) and the Trident data.

While the property maps may explain the sense of the west to east salinity change, they fail to clarify why the front occurs at 60W. The salinity gradient in the upper and lower thermocline is caused by different phenomenon so it is unlikely that both fronts should be aligned within the water column. Also, a gradual increase in salinity

toward the east would be expected rather than the sharp increase observed in the data. Fronts often result from advective patterns, which we suspect is the situation in the western subtropical North Atlantic, the circulation pattern being the collision of the energetic Gulf Stream recirculation cell with the sluggish Sverdrup interior flow. The front results from a lack of exchange of water properties across the gyre's boundaries (Rhines and Holland, 1982). The higher salinity water from the interior and the fresher recirculation water converge at the gyre's eastern edge where a strong gradient develops. The front is not observed in the Trident nutrient and oxygen data despite there being a strong gradient across the subtropical North Atlantic in both parameters (Reid, 1994). This could be due to the lower dynamic range and nonconservative nature of these tracers.

b. Potential vorticity. Potential vorticity is a conservative tracer along isopycnals except for near the surface where buoyancy flux and wind stress can introduce or remove vorticity. Because it is conservative, the potential vorticity within an unventilated gyre is eventually homogenized through the intra-gyral diffusion of properties (Rhines and Holland, 1982). This is observed in models (Luyten *et al.,* 1983) and in the hydrographic data of the subtropical North Atlantic (McDowell *et al.,* 1982) where a region of constant potential vorticity is found within the recirculation gyre. If the front revealed by the Trident data mark the boundary of the Gulf Stream recirculation, they should be located at the edge of a uniform vorticity region, which is indeed the case.

The vertical potential vorticity (q) is obtained from the relation

$$q = \frac{(f + \omega)}{\rho} \frac{\delta\rho}{\delta z}.$$

Here ω is the relative vorticity and f is the planetary vorticity ($2\Omega \cos \theta$). To calculate q from the Trident hydrographic data, ω was assumed to be negligible relative to f, and the calculations were done using $\delta z = 10$ decibars. A Gaussian filter was then applied along z and the potential vorticity plotted with σ_θ as the vertical coordinates.

In the northern section (Fig. 8a) the STMW can be distinguished as a q-min between $\sigma_\theta = 26.3$ and 26.5 (McCartney, 1982). As noted previously, the STMW weakens at 60 W, where the recirculation front is observed. The water below the STMW is marked by a q-max in the west, defined by the $q = 12$ contour. Except for a slight decrease in the vorticity near 72W, the vorticity in the q-max is greater than $q = 12$ throughout. East of 60W the vorticity sharply decreases and, except for an anomaly near 54W, is less than $q = 11$. A plot of the vorticity on an isopycnal reveals that the vorticity does not vary much within the q-max region, as expected if this was part of an unventilated gyre. Between the 26.7 and 27.2 isopycnals the vorticity is generally between $q = 12$ and 14. East of the front the vorticity varies more, from $q =$ 5 to 13. The q-max water is found throughout the main and lower thermocline

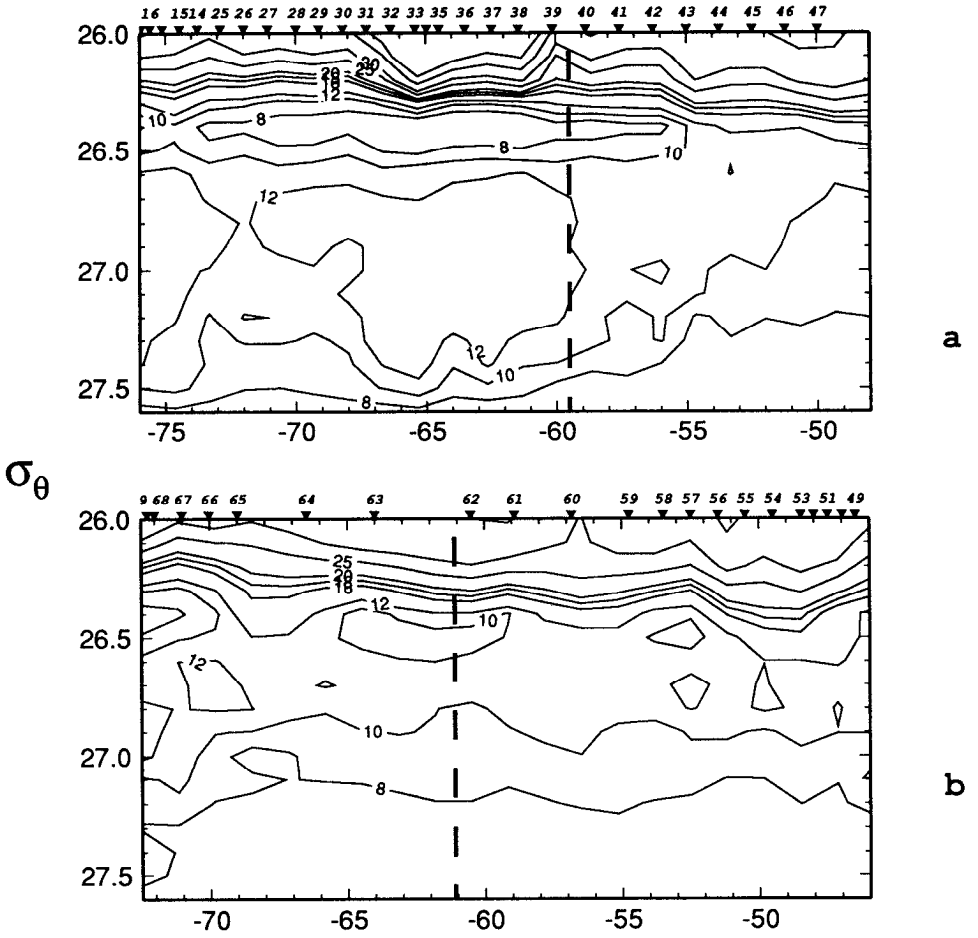

Figure 8. Smoothed potential vorticity of the Trident 1992 data for the northern (a) and southern (b) section with σθ as the ordinate. The contours have the units 10^{-13} cm^{-1} sec^{-1}.

suggesting that vertical diffusivity of potential vorticity within the gyre occurs, homogenizing the potential vorticity in the vertical as well as the horizontal. East of the recirculation front the potential vorticity contours are inclined relative to density surfaces as the q-min and q-max disappear.

In the southern section (Fig. 8b) the q-min indicative of the STMW, and the q-max are significantly reduced. This section is near the southern edge of the recirculation gyre (Reid, 1994) and part of the flow consists of ventilated thermocline water advected westward from the interior. The q contours are generally parallel to the isopycnals indicating possible zonal flow, since stream lines follow lines of constant q along isopycnals.

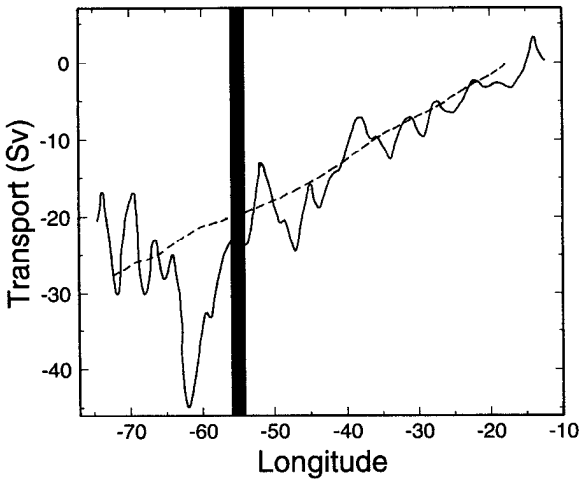

Figure 9. Geostrophic transport (bold solid line) above $\sigma_\theta = 27.4$ with wind driven geostrophic transport (dashed line) calculated using mean annual wind stress data of (Hellerman and Rosenstein, 1983). The transports are integrated from the eastern boundary. (From Roemmich and Wunsch, 1985, Fig. 13a).

c. Atlantis II 1981 sections. The recirculation front with characteristics similar to those observed in the Trident data is detected in two 1981 RV *Atlantis* II transatlantic sections (Roemmich and Wunsch, 1985, hereafter RW 85). The northern section crosses the Atlantic at 36.25N, the southern section at 24.5N. RW 85 calculate the geostrophic transport for water above $\sigma_\theta = 27.4$ and compare it to the Sverdrup calculated transport using the Hellerman and Rosenstein (1983) mean wind stress data. They find that in the southern section the geostrophic transport and the Sverdrup transport are closely correlated east of 56W. West of 56W, the transports diverge with the geostrophic transport having a strong southerly component between 56 and 66W in excess of the Sverdrup transport (Fig. 9). It can be inferred from this that 56W marks the boundary between the recirculation gyre and the interior Sverdrup regime. The Atlantis potential vorticity field also verifies the edge of the recirculation in the southern section with a q-max ($q = 12 \times 10^{-13}$ cm^{-1}/s^{-1}) in the main and lower thermocline which extends east to 55W. On the 36N line, the eastern edge of the recirculation cell is located near 46W.

Both 1981 sections experience a jump in upper thermocline salinity at the eastern edge of the recirculation. Because the 36N section is north of the high salinity maximum, there is, instead, a freshening to the east of the gyre's edge (RW 85, Fig. 3c). In the lower thermocline both sections show an increase in salinity to the east. At 24N the salinity characteristics on the 10°C isotherm (Fig. 10a) change between 63W and 55W, a slight jump occurring at both points. West of 67W the salinity is constant near 35.31. East of 55W the salinity is everywhere greater than 35.34 and increases to the east. Between 55 and 67W there is a salinity plateau that

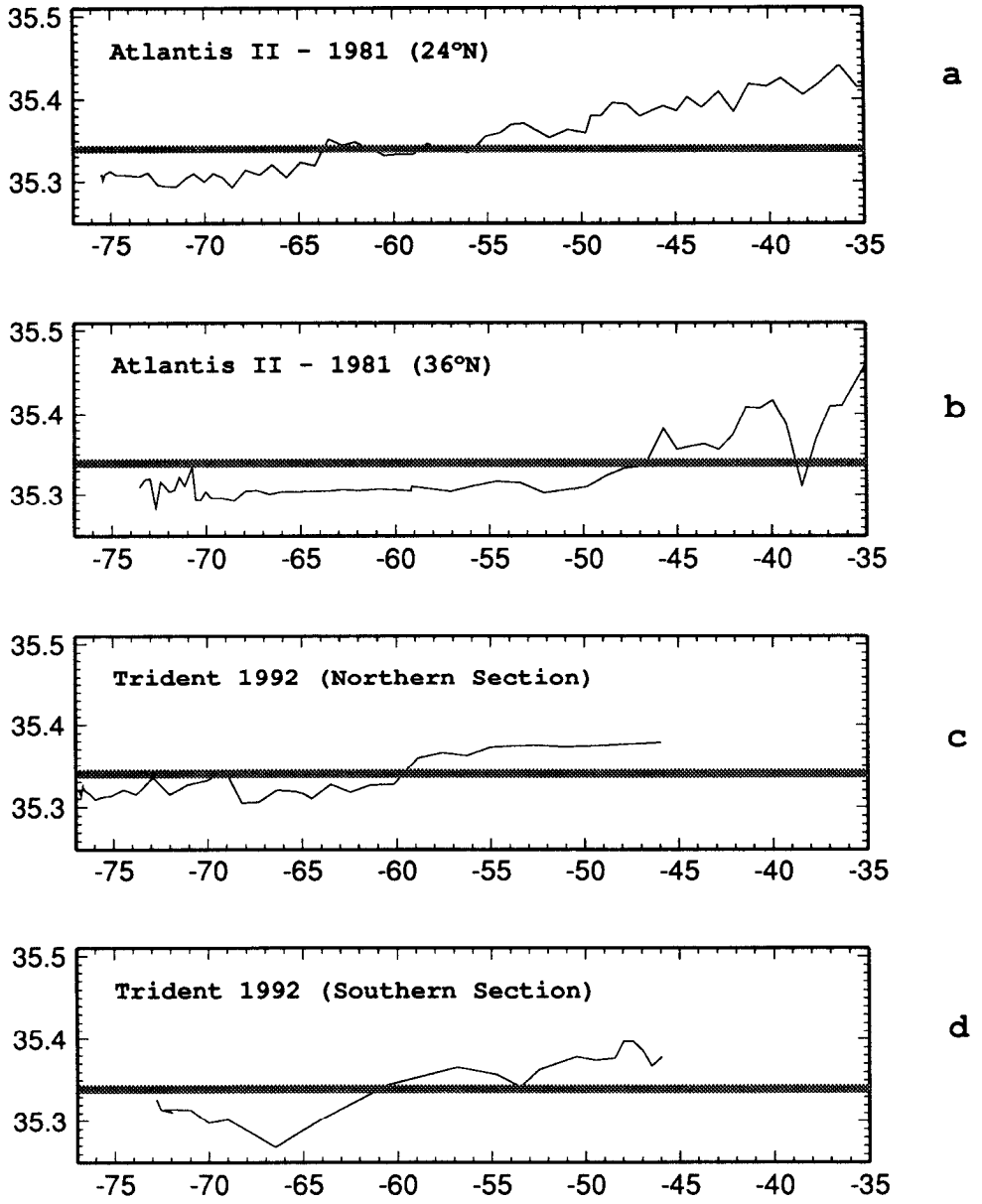

Figure 10. Salinity on the 10°C isotherm for the *Atlantis II* (1981) data—24N line (a), 36N line (b), Trident 1992—northern section (c), Trident 1992—southern section (d).

could result if this part of the section follows along the front, indicating that the front may not always have a meridional alignment. In the northern section (Fig. 10b) the salinity within the recirculation region is constant between 35.3 and 35.32. At 46W there is a sharp increase in the salinity to the east.

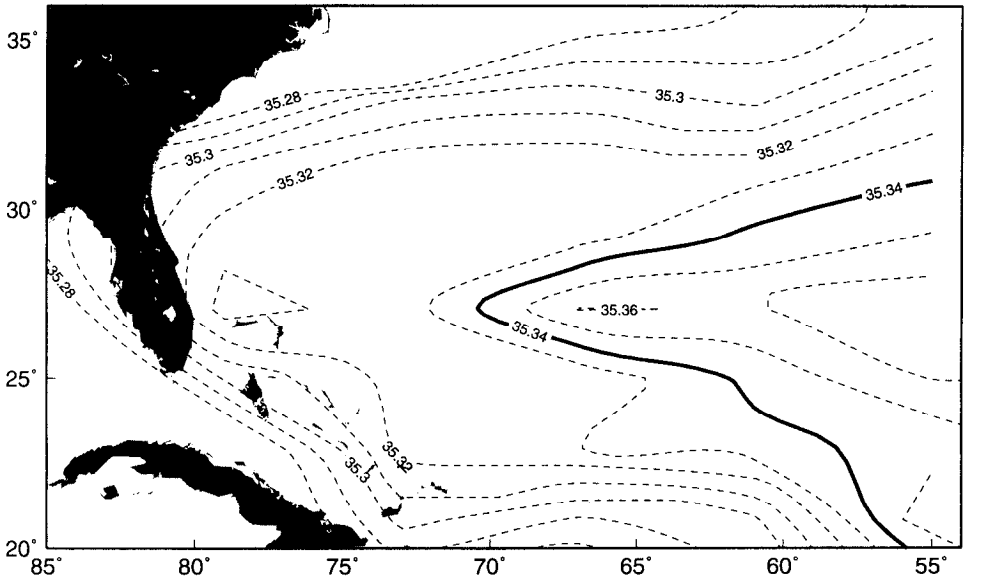

Figure 11. Salinity on the 10°C isotherm. Map compiled from the Trident and Joe Reid data set.

d. Mapping the recirculation front. The recirculation front is observed in other data sets where a salinity jump is present in the upper and lower thermocline between 60 and 70W. However, the front is not always as distinct or in the same position as it is in the Trident data, possibly because the recirculation's size and intensity vary with time (Schmitz and McCartney, 1982). Using archived hydrographic data and constructing a salinity map for the 10°C isotherm (Fig. 11) reveals a region in the western subtropical North Atlantic with nearly constant salinity. Between 60 and 70W, near the 35.34 isohaline, the salinity sharply increases forming a continuous C-shaped front with a wedge of high salinity water intruding west at 27N. This is the high salinity wedge discussed by Reid (1978) to propose the C-shaped circulation pattern in this region.

That the location of the recirculation front coincides with previous recirculation schemes derived from dynamic height data (Stommel *et al.,* 1978; Schmitz and McCartney, 1993) is not surprising since a strong geostrophic shear will occur at the front. The location of the recirculation front also coincides with the eastern limit of floats released within the recirculation gyre (Owens, 1991).

4. Discussion

A thermocline front is observed in the subtropical North Atlantic that marks the eastern edge of the Gulf Stream recirculation gyre. This is supported by the water mass distribution (Section 2 and 3a), the potential vorticity field (Section 3b), and the

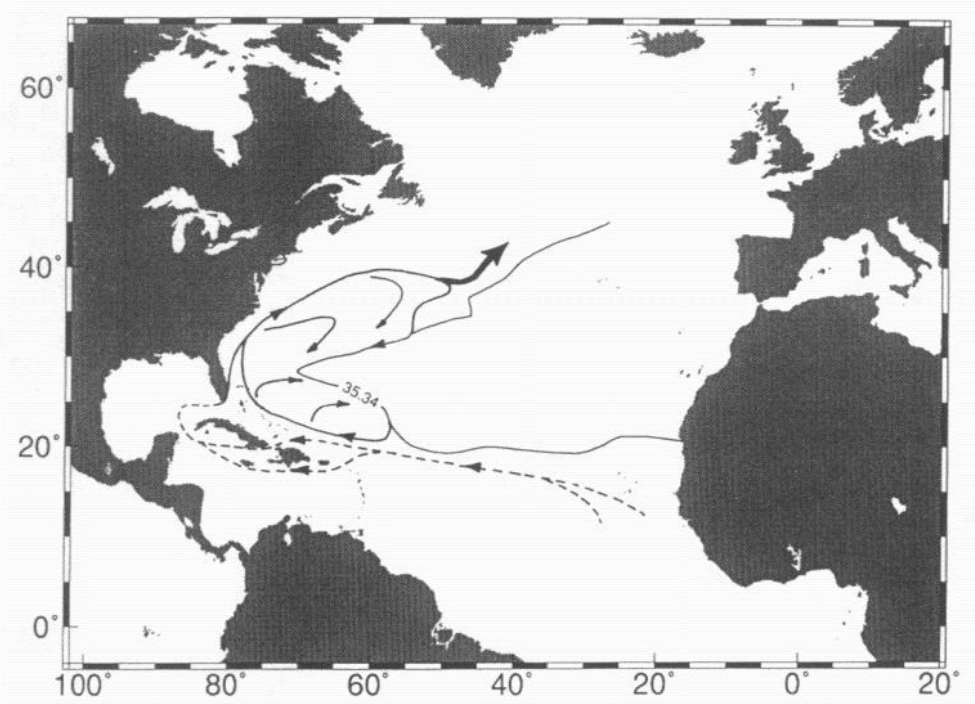

Figure 12. The recirculation front with a proposed circulation scheme for the recirculation gyre superimposed so that the eastern edge of the recirculation coincides with the position of the recirculation front.

transport calculations of RW 85 (Section 3c) which show that the meridional geostrophic transport and wind calculated transport diverge where the front occurs. The Trident geostrophic velocities relative to a deep reference level proved inconclusive and are not included in the analysis. Using the historical hydrographic data to recreate the salinity field for the North Atlantic reveals a C-shaped continuous front following the shape of the dynamic topography expression of the Gulf Stream circulation gyre. The isohaline 35.34 on the 10°C isotherm may be used to locate the front.

The possibility that a salinity front resides at the edge of the recirculation cell has been proposed previously. Ebbesmeyer and Taft (1979) detected a front across a meridional section which they suggested was located at the recirculation's edge. It is now verified that a continuous front is found throughout the eastern boundary of the Gulf Stream recirculation. The wedge of high salinity water which gives it the distinct C-shape of the recirculation gyre penetrates as far west as 70W. This is where the majority of the subtropical convergence zone (STCZ) fronts have been observed in the North Atlantic.

The occurrence of fronts in the western STCZ has been extensively studied (Voorhis and Hersey, 1964; Katz, 1968; Colton *et al.*, 1975; Pollard, 1986; Halliwell

and Cornillon, 1989; Halliwell *et al.,* 1991; Eriksen *et al.,* 1991) and attributed to Ekman convergence (Roden, 1975). That the recirculation front extends into the STCZ brings up the possibility that some of the fronts observed in the STCZ, and attributed to Ekman convergence, result instead because of the recirculation. It could also be that the recirculation gyre is influenced by the wind stress pattern so that at some locations the recirculation front and STCZ fronts coincide. Theoretically, because the STCZ fronts result from Ekman convergence, the feature should be confined to the surface. Because of this, many of the frontal studies in this region focus on the upper thermocline. However, careful examination usually reveals a front in the lower thermocline indicative of the recirculation front.

Another feature of the STCZ is the occurrence of dual zonal fronts several degrees latitude apart. Double fronts are observed by Voorhis and Hersey (1964) in their section from Eleuthera to Bermuda, can be seen in the FASINEX data (Weller, 1991), and detected by Miller and McCleave (1994) in their analysis of ocean biology. Ekman convergence theory does not explain the occurrence of the second front. It is possible that the fronts are individual manifestations of the Ekman and recirculation fronts. A more likely scenario is that the fronts are caused by the recirculation when it doubles back and forms the wedge near 27N.

Acknowledgments. We are indebted to the officers and crew of the NOAA research vessel *Malcolm Baldrige* and to our colleagues at the NOAA Atlantic Oceanographic and Meteorological Laboratory for their help in collecting the data. This work was supported by NOAA grant no. NA46GP0109. This is Lamont-Doherty Earth Observatory contribution 5463.

REFERENCES

Broecker, W. S., T. Takahashi and Y. K. Li. 1976. Hydrography of the central Atlantic-I. The two-degree discontinuity. Deep-Sea Res., *23,* 1083–1104.

Cessi, P., G. Ierley and W. Young. 1987. A model of the inertial recirculation driven by potential vorticity anomalies. J. Phys. Oceanogr., *17,* 1640–1652.

Colton, J. B., D. E. Smith and J. W. Jossi. 1975. Further observations on a thermal front in the Sargasso Sea. Deep-Sea Res., *22,* 433–439.

Csanady, G. T. and J. L. Pelegri. 1995. Vorticity balance of boundary currents. J. Mar. Res., *53,* 171–187.

Ebbesmeyer, C. C. and B. A. Taft. 1979. Variability of potential energy, dynamic height and salinity in the mean pycnocline of the western North Atlantic. J. Phys. Oceanogr., *9,* 1073–1089.

Eriksen, C. C., R. A. Weller, D. L. Rudnick, R. T. Pollard and L. A. Regier. 1991. Ocean frontal variability in the Frontal Air-Sea Interaction Experiment. J. Geophys. Res., *96* (C5), 8569–8591.

Gunn, J. T. and D. R. Watts. 1982. On the currents and water masses of the Antilles/Bahamas arc. J. Mar. Res., *40,* 1–18.

Halliwell, G. R. and P. Cornillon. 1989. Large-scale SST anomalies associated with subtropical fronts in the western North Atlantic during FASINEX. J. Mar. Res., *47,* 757–775.

Halliwell, G. R., P. Cornillon, K. H. Brink, R. T. Pollard, D. L. Evans, L. A. Regier, J. M. Toole and R. W. Schmitt. 1991. Descriptive oceanography during the Frontal Air-Sea

Interaction Experiment: medium- to large-scale variability. J. Geophys. Res., *96*(C5), 8553–8567.

Hellerman, S. and M. Rosenstein. 1983. Normal monthly wind stress over the world ocean with error estimates. J. Phys. Oceanogr., *13,* 1093–1104.

Hogg, N. G., R. S. Pickart, R. M. Hendry and W. J. Smethie. 1986. The northern recirculation gyre of the Gulf Stream. Deep-Sea Res., *33,* 1139–1165.

Huang, R. X. 1990. Does atmospheric cooling drive the Gulf Stream recirculation? J. Phys. Oceanogr., *20,* 750–757.

Katz, E. 1968. Further study of a front in the Sargasso Sea. Tellus, *XXI,* 259–269.

Kawase, M. and J. L. Sarmiento. 1986. Circulation and nutrients in mid-depth Atlantic waters. J. Geophys. Res., *91*(C8), 9749–9770.

Lee, T. N., W. Johns and F. Schott. 1990. Western boundary current structure and variability east of Abaco, Bahamas at 26.5N: J. Phys. Oceanogr., *20,* 446–466.

Luyten, J., J. Pedlosky and H. Stommel. 1983. The ventilated thermocline. J. Phys. Oceanogr., *13,* 292–309.

McCartney, M. S. 1982. The subtropical recirculation of mode waters. J. Mar. Res., *40*(Suppl.), 427–464.

McDowell, S. 1982. North Atlantic potential vorticity and its relation to the general circulation. J. Phys. Oceanogr., *12,* 1417–1436.

Miller, J. M. and J. D. McCleave. 1994. Species assemblages of leptocephali in the Subtropical Convergence Zone of the Sargasso Sea. J. Mar. Res., *52,* 743–772.

Owens, W. B. 1984. A synoptic and statistical description of the Gulf Stream and the subtropical gyre using SOFAR floats. J. Phys. Oceanogr., *14,* 104–113.

—— 1991. A statistical description of the mean circulation and eddy variability in the northwestern Atlantic using SOFAR Floats. Prog. Oceanogr., *28,* 257–303.

Owens, W. B., J. R. Luyten and H. L. Bryden. 1982. Moored velocity measurements on the edge of the Gulf-Stream recirculation. J. Mar. Res., *40*(Suppl.)., 509–524.

Pollard, R. 1986. Frontal surveys with towed profiling conductivity/temperature/depth measurement package (SeaSoar). Nature, *323,* 433–435.

Reid, J. 1994. On the total geostrophic circulation of the North Atlantic Ocean: Flow patterns, tracers, and transports. Prog. Oceanogr., *33,* 1–92.

—— 1978. On the mid-depth circulation and salinity field in the North Atlantic Ocean. J. Geophys. Res., *83*(C10), 5063–5067.

Rhines, P. B. and W. R. Holland. 1982. Homogenization of potential vorticity in planetary gyres. J. Fluid. Mech., *122,* 347–368.

Richardson, P. L. 1985. Average velocity and transport of the Gulf Stream near 55W. J. Mar. Res., *43,* 83–111.

Roden, G. I. 1975. On North Pacific temperature, salinity, sound velocity and density fronts and their relation to the wind and energy flux fields. J. Phys. Oceanogr., *5,* 557–571.

Roemmich, D. and C. Wunsch. 1985. Two transatlantic sections: meridional circulation and heat flux in the subtropical North Atlantic Ocean. Deep-Sea Res., *32,* 619–664.

Schmitt, R., P. S. Bogden and C. E. Dorman. 1989. Evaporation minus precipitation and density fluxes for the North Atlantic. J. Phys. Oceanogr., *19,* 1208–1221.

Schmitz, W. 1980. Weakly depth-dependent segments of the North Atlantic circulation. J. Mar. Res., *38,* 111–133.

Schmitz, W. J. and M. S. McCartney. 1982. An example of long-term variability for subsurface current and hydrographic patterns in the western North Atlantic. J. Mar. Res., *40* (Suppl.), 707–726.

—— 1993. On the North Atlantic circulation. Rev. Geophys., *31,* 29–49.
Schmitz, W. J. and P. L. Richardson. 1991. On the sources of the Florida Current. Deep-Sea Res. *38* (Suppl.), S379–S409.
Spall, M. A. 1992. Cooling spirals and recirculation in the subtropical gyre. J. Phys. Oceanogr., *22,* 564–571.
Stommel, H., P. Niiler and D. Anati. 1978. Dynamic topography and recirculation of the North Atlantic. J. Mar. Res., *36,* 449–468.
Sverdrup, H. U., M. W. Johnson, and R. H. Flemming. 1942. The Oceans: Their Physics, Chemistry and General Biology, Prentice Hall, 1087 pp.
Talley, L. D. and M. R. Raymer. 1982. Eighteen degree water variability. J. Mar. Res., *40*(Suppl), 757–775.
Tsuchiya, M. 1989. Circulation of the Antarctic Intermediate Water in the North Atlantic Ocean. J. Mar. Res., *47,* 747–755.
Voorhis, A. D. and J. B. Hersey. 1964. Oceanic thermal fronts in the Sargasso Sea. J. Geophys. Res., *69*(18), 3809–3814.
Weller, R. A. 1991. Overview of the Frontal Air-Sea Interaction Experiment (FASINEX): A study of the air-sea interaction in a region of strong oceanic gradients. J. Geophys. Res., *96*(C5), 8501–8516.
Worthington, L. V. 1959. The 18° water in the Sargasso Sea. Deep Sea Res., *5,* 297–305.
—— 1972. Negative oceanic heat fluxes as a cause of water-mass formation. J. Phys. Oceanogr., *2,* 205–211.
—— 1976. On the North Atlantic Circulation. Johns Hopkins Oceanographic Studies, *VI,* The Johns Hopkins University Press, 110 pp.
Wright, W. R. 1970. Northward transport of Anarctic Bottom Water in the western Atlantic Ocean. Deep-Sea Res., 17, 367–371.
Wüst, G. 1963. On the stratification and the circulation in the cold water sphere of the Antillean-Caribbean basins. Deep-Sea Res., *10,* 165–187.

Received: *7 September, 1995;* revised: *14 December, 1995.*